ZIBELINE INTERNATIONAL PUBLISHING

ISSN: 2521-5035 (Print)
ISSN: 2521-5043 (Online)
CODEN: ESMACU

Earth Sciences Malaysia (ESMY)

DOI: http://doi.org/10.26480/esmy.02.2020.127.134

RESEARCH ARTICLE

GEOCHEMICAL CHARACTERISTICS OF GOLD-BEARING GRANITOIDS AT AYANFURI IN THE KUMASI BASIN, SOUTHWESTERN GHANA: IMPLICATIONS FOR THE OROGENIC RELATED GOLD SYSTEMS

Theophilus K. Agbenyezi*, Gordon Foli, Simon K. Y. Gawu

Department of Geological Engineering, Kwame Nkrumah University of Science and Technology (KNUST).
****Corresponding Author Email: kekelitheophilus@gmail.com***

ARTICLE DETAILS

Article History:

Received 01 March 2020
Accepted 30 May 2020
Available online 23 June 2020

ABSTRACT

This study investigates auriferous granitoids from the Esuajah and Fobinso pits within the Ayanfuri environment in the Paleoproterozoic Kumasi basin. The aim is to establish the geochemical characteristics of the granitoid gold ores and the possible deposit type which may influence mineral project development. 13 major and 51 trace elements were analyzed using XRF and ICP-MS devices, respectively. The granitoids are mainly classified as granodiorite that crystallized from a calc-alkaline magma series. The Fobinso granodiorite derived from the partial melting of the Birimian metasedimentary rocks, while the Esuajah granitoid derived from igneous rock melts. The granitoid are linked to magma source depleted in mantle material that contains crustal components through subduction processes. Major oxides of the granitoid vary lowly from the average background values derived for basin type granitoid in such terrains. Generally, the granitoid are enriched in Large Ion Lithophile Elements (LILE), while High Field Strength Elements (HFSE) and base metals are within background values when compared to Primitive Mantle (PM) values. Gold mineralisation is associated with Ag, As, Bi, Sb, Te, Pb and S in the peraluminous granitoids. Geochemical characteristics and field observations identify the deposit style as an orogenic related gold deposit type.

KEYWORDS

Esuajah granitoids, Lithophile Elements, Fobinso granodiorite, calc-alkaline magma, peraluminous.

1. INTRODUCTION

Until the revival of gold exploration in Ghana in the late 1980s, only two major types of gold deposit types were extensively studied within the Birimian metallogenic province in Ghana (Yao and Robb, 2000). These deposit types are the shear zone hosted lode-quartz veins and/or disseminated sulphides and the auriferous quartz-pebble conglomerates (Kesse, 1985; Hirdes and Leube, 1989; Leube et al., 1990 and Schmidt Mumm et al., 1997).

Extensive exploration works in the Birimian terrain of Ghana have led to the discovery of gold-bearing granitoid, which constitute a third and recent style of gold mineralization in the Birimian (Yao et al., 2001). The earliest notable occurrence of gold-bearing granitoid in the Birimian of Ghana was at Ayanfuri, where several of the deposits are hosted by intermediate to felsic granitoid that have significant mineralized quartz stockwork systems (Griffis et al., 2002).

For several decades, gold exploration has been mainly focused on sediment-hosted shear zones, where significant deposits have in time past formed the basis of gold exploitation. Currently, however, Gold deposits hosted within the Birimian granitoid are increasingly becoming potential targets for exploration to maximise the gold ore resource base to aid increased productivity. Examples of the granitoid bodies identified for study include the Ayanfuri, Nhyiaso, and Ayankyerim, gold deposits in the western part of the Ashanti Belt, the Chirano gold deposits in the Sefwi Belt (Fougerouse et al., 2017; Allibone et al., 2004). Also, of interest is the Dynamite Hill and Abore gold deposits along a 10-20 km wide shear zone within the Kumasi Basin and equidistant from the Sefwi and Ashanti Belts (Chudasama et al., 2016).

Although the Ashanti style mineralization occurs with gold-bearing granitoid in the study area, mineralized intrusions have been the main attraction at the Ayanfuri and its environs (Calderwood and Thompson, 2007). There is, however, only very little in terms of geological characterisation of these deposits (Griffis et al., 2002). Emplacement of granitic plutons in the sedimentary basins is coeval with the tectono-thermal orogeny that is constrained to the time range of 2120 -2080 MY (Oberthur et al., 1998). Orogenic deposits are formed during crustal shortening in compressional deformation processes within metamorphosed terranes with consequent generation of large volumes of granitic melts (Grooves et al., 2003; Grooves et al., 1998).

Differences between orogenic gold-bearing granitoids and the intrusion-related gold deposits remain unresolved (Sillitoe, 1991). This is because the two deposit types have many similarities in terms of element

Quick Response Code	Access this article online	
	Website: www.earthsciencesmalaysia.com	DOI: 10.26480/esmy.02.2020.127.134

Cite the Article: Theophilus K. Agbenyezi, Gordon Foli, Simon K. Y. Gawu (2020). Geochemical Characteristics Of Gold-Bearing Granitoids At Ayanfuri In The Kumasi Basin, Southwestern Ghana: Implications For The Orogenic Related Gold Systems. *Earth Sciences Malaysia, 4(2): 127-134.*

associations, ore fluids wall-rock alteration and structural controls (Goldfarb, 2001; Grooves et al., 2003). Consequently, some gold-bearing granitoids have been classified as both orogenic and intrusion-related deposits that includes the Muruntau gold deposits of Uzbekistan and the True North deposit in Canada (Kempe et al., 2001; Hart et al., 2000). With the different approaches to gold exploration associated with the intrusion-related and orogenic gold classifications, it is pertinent to suitably identify each model (Hart and Goldfarb, 2005).

The Birimian Supergroup in the Kumasi basin comprises metasedimentary rocks, metavolcanic rocks, and basin type granitoid that intruded the basin sequences from c. 2,116 to 2,088 Ma (Adadey et al., 2009). The metasedimentary units consist of greywackes, graphitic shale, and argillaceous sediments, while the metavolcanic rocks generally include basalt, dacite and rhyolite (Hirdes and Davis, 2002). The metasedimentary country rocks are intruded by dykes and small irregular plugs of granitoid (Tourigny et al., 2018). The rocks are intensely folded, faulted and metamorphosed to upper greenschist facies during regional metamorphism ascribed to the Eburnean orogeny (Hirdes and Davis, 2002). The gold deposition is associated with granitoid bodies, and shear zones within the Birimian. In this study, major elements classification and trace elements geochemistry are used to constrain the deposit type of the granitoids, which have only been studied sparingly, either on an individual basis or regional basis (Yao et al., 2001). For an enhanced modeling and exploration approach in the study area, a more detailed understanding of the nature and origin of the granitoid and their associated gold mineralization is required. The study assessed auriferous granitoid suites from the Esuajah granitic plug and Fobinso dyke in Ayanfuri of the Kumasi Basin.

2. Materials and Methods

2.1 Study area

The study area is situated within the Kumasi basin, near the western flank of the Ashanti Greenstone Belt, at the extreme south-eastern portion of the West African Craton and underlain by the tectonostratigraphic Leo Man shield (Jessell et al., 2016). Rocks are dominated by the Paleoproterozoic Birimian rocks of Eburnean age (Leube et al., 1990) (Figure 1). A sketched local geological map is presented in Figure 2.

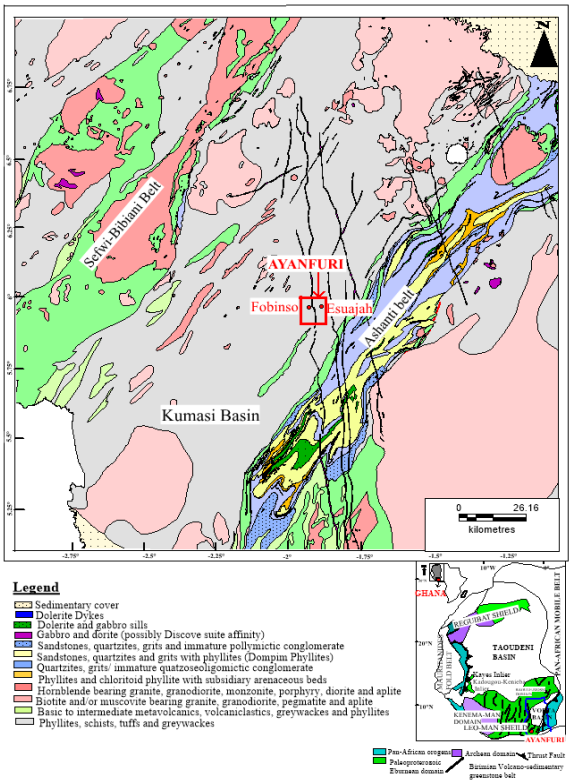

Figure 1: Simplified geological map showing the location of Ayanfuri in southwestern Ghana (modified after Perrouty et al., 2012)

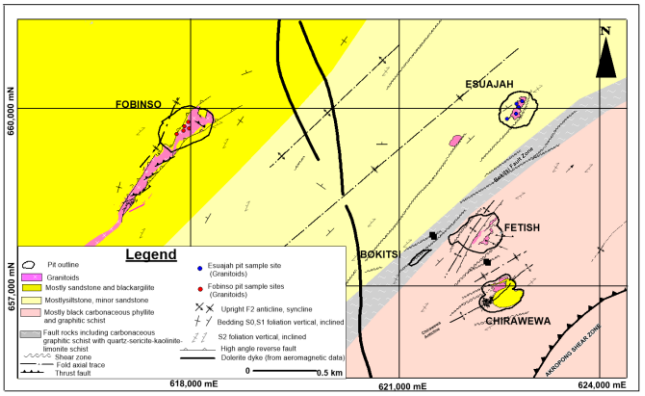

Figure 2: Geological and structural setting of the gold deposit cluster at Ayanfuri (modified after Tourigny et al., 2018)

The Esuajah gold deposit is hosted in cylindrical granitoid plug whereas the Fobinso gold deposit is contained in a single, continuous dyke (Tourigny et al., 2018). The granitoid hosted gold deposits are associated with lesser arsenopyrite and traces of sphalerite, chalcopyrite, galena and rutile. Very fine-grained gold occurs along sulphide grain boundaries and in fractures in sulphide crystals (CAGL, 2011). The study area is well noted for historic mining activities (Griffis et al., 2002). Esuajah and Fobinso open pits of metasediment hosting auriferous intrusive were the main source of rock samples for the study (Figure 2). The pits are barren of saprolite as old mine workings focused much of their activities on oxide material leaving behind competent in-situ rock exposures with strongly preserved primary and secondary structures.

2.2 Sampling strategy and procedure

Pre-sampling mapping of pit walls was carried out to identify prevailing lithology and structures in the various pits as they are major factors controlling mineralization. Representative and fresh samples were carefully taking from intrusives at Fobinso and Esuajah pits. Samples were taken from chloritic and sericite alterations zones, veins crosscutting granitoid intrusions (Figure 3), as well as altered granitoids with disseminated sulphides.

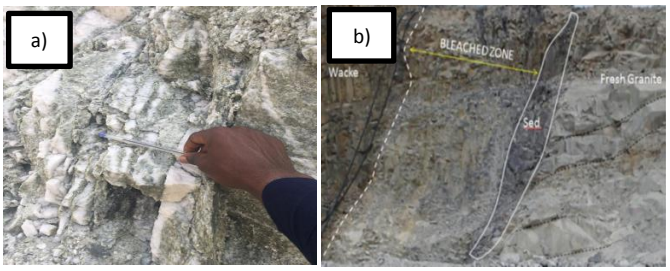

Figure 3: a) The granitic intrusion at Esuajah North Pit showing steeply dipping veins. b) Lithological contact of mineralized granite and the intruded basinal sediments at Fobinso.

All the samples are coarse-grained and partially altered. Sample locations and field descriptions are presented in Table 1.

Table 1: Field description and sample locations.

Samp_ID	Northings	Eastings	Field description
E12/0401	660114	622876	~10% Quartz, Chlorite and Sericite alterations
E12/0402	660073	622796	~ 5% Pyrite and Chlorite Alteration
E12/0403	660011	622825	~ 1% Pyrite
E12/0404	659903	622787	~1 % Pyrite and Asenopyrite
E12/0405	659810	622650	~10% Asenopyrite
F12/0401	659768.55	617879.59	>1% sulphides
F12/0402	659654.32	617890.26	Sericite Alteration
F12/0403	659694.42	617820.08	~ 1% Pyrite
F12/0404	659620.68	617805.46	Sericite Alteration
F12/0405	659557.83	617700.11	~5% Pyrite

A total of 10 samples were selected for determination for major elements and selected trace elements including gold. Samples were packaged and dispatched to the ALS Geochemical Laboratory for chemical analyses. Analytical methods used are inductively coupled plasma mass spectrometry (ICP-MS), inductively coupled plasma atomic emission spectrometry ICP-AES and X-Ray Fluorescence. Elements analyzed with XRF include SiO_2, TiO_2, Al_2O_3, total Fe as Fe_2O_3, MnO, MgO, CaO, Na_2O, K_2O, P_2O_5, BaO, SrO and Cr_2O_3. The trace elements analyzed with ICP-MS and ICP-AES includes Ag, Al, As, Au, B, Ba, Be, Bi, Ca, Cd, Ce, Co, Cr, Cs, Cu, Fe, Ga, Ge, Hf, Hg, In, K, La, Li, Mg, Mn, Mo, Na, Nb, Ni, P, Pb, Rb, Re, S, Sb, Sc, Se, Sn, Sr, Ta, Te, Th, Ti, Tl, U, V, W, Y, Zn and Zr.

Chemical analysis was done on about 5.0 g of sample portions each, using the X-ray fluorescence (XRF) as described (Wirth and Barth, 2016). Also, the volatile content of each sample was determined by loss on ignition (LOI), as summarized (Santisteban et al., 2004). The concentrations of the elements and the LOI values were reported in percentages and part per million for major oxides and trace elements respectively. A model-based ordinary and robust Expectation-Maximisation algorithms outlined was used to generate element concentrations below the detection limit of analytical equipment (Palarea-Albaladejo et al., 2007; Martin-Fernandez et al., 2012). Data replacement was done using the R package zCompositions. The Centered log-ratio (clr) transformation proposed was used to open the constrained compositional data to reveal inherent patterns in the data structure using the expression (Aitchison, 1982):

$$clr(x) = [\log\{x_1/g(x)\} \ldots, \log\{x_N/g(x)\}] \quad (1)$$

where x represents the composition vector, g(x) is the geometric mean of the composition x, and x_1, ..., x_N are the concentrations of the individual elements. The R Package Geochemical Data Toolkit (GCDkit) was used to plot classification diagrams for the granitoids (Janoušek et al., 2016).

3. Results and Discussion

3.1 Geochemical Characteristics

Table 2 presents the analytical data for each rock type from Esuajah and Fobinso intrusions.

Table 2: Whole-rock major (wt %) and trace (ppm) element compositions of granitoids from Ayanfuri

Samples	F12/0401	F12/0402	F12/0403	F12/0404	F12/0405	E12/0401	E12/0402	E12/0403	E12/0404	E12/0405
SiO_2	67.7	70	67.7	67.9	65	68.1	68.5	68.7	67.7	73
TiO_2	0.28	0.26	0.3	0.31	0.32	0.26	0.27	0.3	0.27	0.25
Al_2O_3	15.1	14.95	15.9	15.8	22	14.75	15	14.6	14.45	13.95
Fe_2O_3t	2.94	2.49	2.82	2.57	1.53	2.73	2.76	2.71	2.8	1.32
MnO	0.03	0.02	0.02	0.02	0.02	0.03	0.03	0.02	0.03	0.01
MgO	0.76	0.69	0.68	0.71	0.61	0.87	0.78	0.76	0.78	0.23
CaO	2.45	1.86	2.36	1.96	2.48	2.66	1.92	2.28	2.38	1.4
Na_2O	4.8	4.98	4.6	5.1	3.5	4.9	4.98	4.99	5.4	5.9
K_2O	1.49	1.36	1.45	1.34	2.64	1.47	2.04	1.19	1.45	1.1
P_2O_5	0.08	0.07	0.08	0.07	0.13	0.06	0.08	0.14	0.1	0.12
BaO	0.04	0.04	0.04	0.04	0.04	0.04	0.05	0.04	0.04	0.04
SrO	0.05	0.03	0.07	0.05	0.05	0.05	0.03	0.05	0.05	0.03
LOI	3.47	2.31	3.18	3.14	2.5	3.6	3.22	3.7	3.74	3
TOTAL	99.19	99.06	99.2	99.01	100.82	99.52	99.66	99.48	99.19	100.35
Trace Elements										
Ag	0.05	0.08	0.03	0.02	0.24	0.27	0.36	0.05	0.02	0.42
As	141.5	22.5	13	14.3	684	709	968	47.2	64.4	2270
Au	0.08	0.013	0.03	0.01	0.63	0.19	0.42	0.02	0.006	3.4
Be	0.16	0.13	0.13	0.18	0.19	0.2	0.24	0.24	0.25	0.1
Bi	0.06	0.05	0.03	0.03	0.02	0.21	0.52	0.1	0.03	0.21
Cd	0.05	0.02	0.02	0.02	0.02	0.07	0.09	0.06	0.04	0.03
Ce	15.9	18.95	18.8	20.1	19.15	9.72	12.45	12.15	13	15.7
Co	5.3	6	5.5	5	3.1	4.9	6	5.8	5.5	1
Cr	20	18	19	19	6	14	19	15	17	13
Cs	0.64	0.43	1.1	0.7	1.08	0.56	0.94	0.49	0.48	0.32
Cu	13.2	15.4	5.8	3.3	1.7	42	31.5	27.5	16.5	19.4
Ga	2.34	5.15	5.37	4.16	5.09	1.8	2.47	1.83	1.64	1.42
Hf	0.05	0.08	0.03	0.06	0.09	0.08	0.14	0.09	0.12	0.19
In	0.01	0.003	0.001	0.01	0.01	0.01	0.01	0.01	0.01	0.01
La	8.5	10.2	10.1	10.7	10.1	5	6.2	6.2	6.6	8.4
Li	6.7	23.4	28.4	14	1.3	1.3	2.1	2.1	1.5	0.6
Mo	1.56	1.23	1.35	1.28	0.38	3.16	3.59	2.19	2.11	2.17
Nb	0.06	0.04	0.02	0.05	0.04	0.06	0.05	0.06	0.06	0.05
Ni	8.8	7.7	8.7	9.2	4.2	8.6	9.9	9.7	9.8	1.6
Pb	4	5.2	3.1	3.5	3.5	4.8	12.1	4.4	3.4	11
Rb	5.5	5	5.3	6.3	10.8	6.9	10.7	5.5	5.8	3.5
S	0.15	0.02	0.04	0.02	0.18	0.48	0.54	0.27	0.13	0.3
Sb	0.06	0.05	0.006	0.002	0.1	4.37	7.26	0.17	0.13	5.21
Sc	1.1	1	1	1.1	1	1.5	1	1.5	1.7	0.7
Te	0.008	0.01	0.01	0.01	0.25	0.03	0.09	0.01	0.002	0.12
Th	1.3	2	1.7	1.9	1.7	0.9	1.3	1.1	1.1	1.5
Tl	0.03	0.03	0.03	0.04	0.06	0.04	0.06	0.03	0.03	0.02
U	0.33	0.46	0.42	0.38	0.32	0.25	0.4	0.36	0.33	0.31
V	6	8	9	7	9	5	5	5	6	3
W	0.06	0.42	0.03	0.05	0.05	0.08	0.06	0.08	0.05	0.022
Y	1.97	1.57	2.03	2	3.32	2.16	3.98	3.09	2.68	1.58
Zn	44	42	44	44	19	34	43	41	44	12
Zr	1.1	1.4	1.5	1.3	1.7	1.7	2.8	2	2.8	5.1

- F12/0400 – Fobinso samples
- E12/0400 – Esuajah samples

The principal characteristics of the two groups of granitoids are discussed below:

3.1.1 Major Elements

The majority of oxides analyzed show little variations from the average background values of the basin type granitoids except for Na_2O which in both Esuajah intrusive and Fobinso granitoids are higher than background values (Table 3) (Leube et al., 1990).

Table 3: Mean oxides concentration of Ayanfuri granitoids compared with Birimian sedimentary basin granitoids

OXIDES	Esuajah This study	Fobinso This study	Sedimentary basin granitoids (Leube et al., 1990)
SiO_2	69.2	67.66	69.24
TiO_2	0.27	0.294	0.32
Al_2O_3	14.55	16.75	15.05
Fe_2O_3t	2.464	2.47	2.73
MnO	0.024	0.022	0.04
MgO	0.684	0.69	0.97
CaO	2.128	2.222	2.19
Na_2O	5.234	4.596	4.37
K_2O	1.45	1.656	2.58
P_2O_5	0.1	0.086	0.09

From Table 2, the Esuajah granitoid shows silica (SiO_2) content ranging from 67.7 to 73wt%, alumina (Al_2O_3) is between 13.95-15wt%, ferromagnesian oxides (Fe_2O_3 + MgO + MnO + TiO_2) range between 3.79 to 3.89 wt% with only sample E12/0405 recording 1.81 wt %. Total alkali (Na_2O +K_2O) values range from 6.18 to 7.02 wt% and K_2O/ Na_2O ratio from 0.19 to 0.41. CaO in Esuajah granitoids show much variation ranging from 1.4-2.66 wt. Fobinso granitoid do not show much major elements variation from the Esuajah granitoid, except for their high K_2O/ Na_2O which ranges from 0.26 to 0.75. Fig. 4 is a Harker plot showing evolution trends of the granitoids.

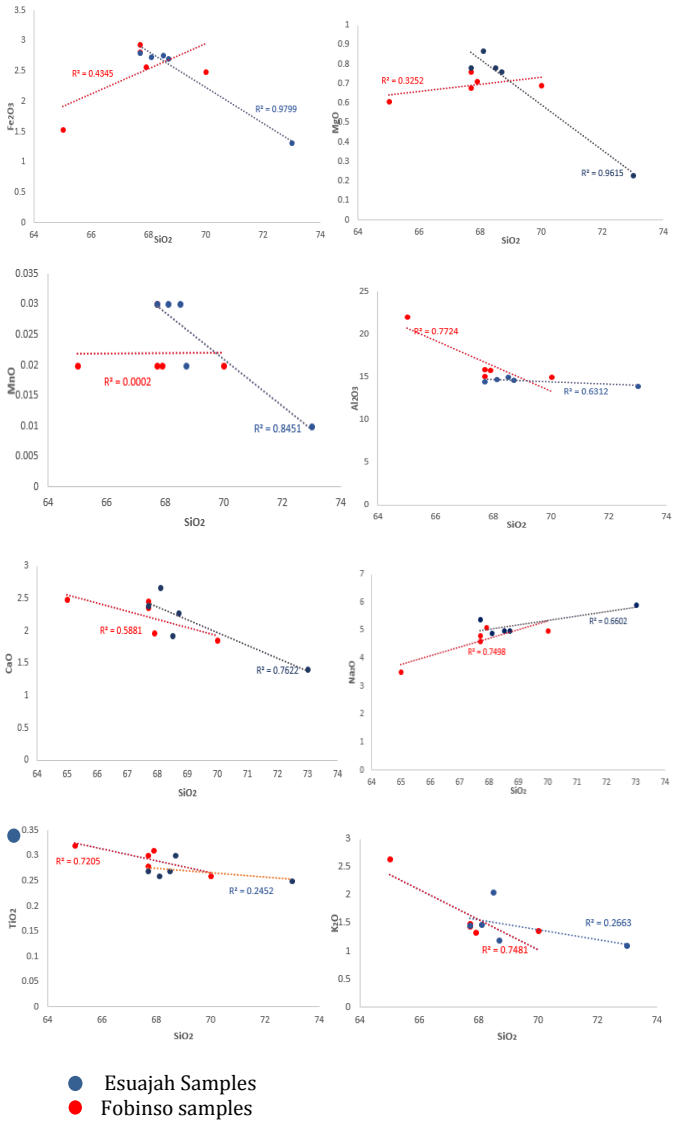

Figure 4: Harker diagrams showing variations of major element oxides with silica for the granitoids

Strong negative and positive correlation coefficients existing between silica and other oxides are indicative of a common formation history of the granitoid (Wilson, 1989). SiO_2 values for Esuajah granitoid show marked inverse correlation with Fe_2O_3 (r= -0.98), MgO (r= -0.96), MnO (r= -0.85), Al_2O_3 (r= -0.63) and CaO (-0.76). While Na_2O shows a positive correlation (r=0.66) with SiO_2. For the Fobinso granitoid, SiO_2 inversely correlates with TiO_2 (r= -0.72), K_2O (r= -0.75), CaO (r= -0.59) and Al_2O_3 (r= -0.77). Negative linear trends of Fe, Mg, Mn and Ti oxides versus SiO2 indicate fractionation of early formed ferromagnesian phases from the precursor magma for the granite.

On the Total Alkalis Silica (TAS) diagram (Figure 5a), The Esuajah and Fobinso granitoid samples plot as granodiorite while some straddle the granodiorite and granite boundary with a few plotting within the granite region. The high content of silica is evident in the TAS diagram as all samples plot in the acid region. The Esuajah intrusive and the Fobinso intrusive are identified to originate from calc-alkaline magma series (Figure 5b) which is a sub-division of the sub-alkaline series (Figure 5a). A subdivision of the calc-alkaline magmas plots the intrusive bodies as a calc-alkaline series member (Figure 5c) (Peccerillo and Talor, 1976).

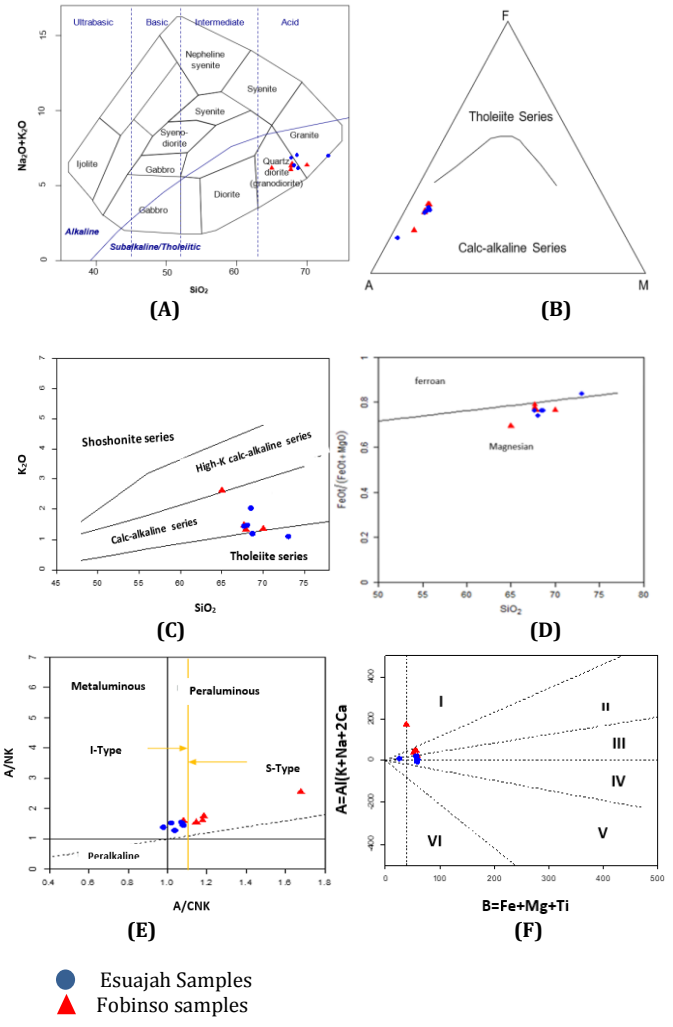

Figure 5: Major elements diagram for Esuajah and Fobinso granitoids. (A) Total alkali vs. silica (TAS) diagram (B) AFM plot Na_2O + K_2O (A), Fe_2O_3* = total Fe expressed as Fe_2O_3 (F), and MgO (M) (C) SiO_2 - K_2O plot (D) SiO_2 vs FeOt/(FeOt + MgO) (E) Shand's molar parameters A/NK = Al_2O_3/(Na_2O+K_2O) vs. A/CNK = Al_2O_3/ (CaO+ Na_2O+K_2O) of the granitoids (Maniar and Piccoli, 1989; Wilson, 1989; Irvine and Baragar, 1971; Peccerillo and Talor, 1976; Frost et al., 2001). Boundary line for I-type and S-type granite field is taken from Chappel and White (2001) (F) Characteristic minerals diagram I-III- Peraluminuous domain (I: muscovite>biotite (by volume), II: biotite>muscovite, III: biotite (usually alone, at times with a few amphiboles)), IV-VI- Metaluminuous domain (IV: biotite + amphibole ± pyroxene, V: clinopyroxene ± amphibole ± biotite, VI: unusual rocks (e.g., carbonatites)) (Debon and Le Fort, 1983).

The Al_2O_3/ ($Na_2O + K_2O$) versus Al_2O_3/ ($CaO + Na_2O + K_2O$) binary diagram (Figure 5e) of Shand deals with discriminating peraluminous, metaluminous and peralkaline magma series (Shand, 1943). This plot shows that all granitoid samples are peraluminous (i.e. Alkalinity index (AI) and Aluminuim Saturation Index (ASI) are greater than one). The peraluminous imprint on samples is indicative of excess aluminium required to form feldspars and can be accommodated in other aluminous phases such as Al_2SiO_5 polymorph (Frost et al., 2001; 2008). The Esuajah granitoid samples plot within the I-type region with a boundary division of ASI >1.1 (Chappel et al., 1974). All samples of Esuajah granitoid have ASI values below 1.1. Four out of five of the Fobinso granitoid samples plot within the S-type region with their ASI values ranging from 1.1 to 1.7, suggesting their S-type affinity. A group of researchers classified the I-type and S-type granites as rocks originating from melts of meta-igneous and metasedimentary material respectively (Chappel et al., 1974). Considering the magnesian nature on the granitic classification diagram (Figure 5d), the anatexis of metasedimentary rocks may have been promoted by hydrous conditions (Frost et al., 2001; Nude et al., 2012).

The peraluminous nature of the samples is again substantiated from the major cation parameters (Figure 5f). The bulk of Ayanfuri intrusive bodies plot in fields II and III which mostly consist of biotite and some amphiboles as the mafic minerals. Biotite is identified to be the main ferromagnesian mineral within the Birimian sedimentary basin type granitoid (Yao, 2000; Nyarko et al., 2012). Granitoid suites plotting within the peraluminous domain are known to be the product of anatexis of continental crust, contrary to the mantle-derived metaluminous domain (Debon and Le Fort, 1983).

3.1.2 Trace elements assessment

To assess trace element behavior of the Fobinso and Esuajah granitoids, the raw multi-element data of the granitic rocks were normalized against Primitive Mantle/Silicate Earth (McDonough and Sun, 1995) and presented in Figure 6.

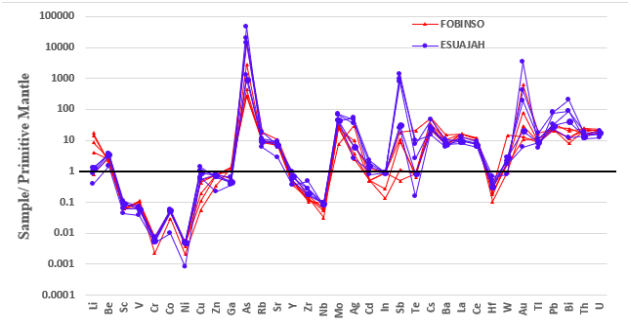

Figure 6: Trace element patterns of Esuajah and Fobinso granitoids normalized to Primitive Mantle/Silicate Earth (McDonough and Sun, 1995)

Esuajah and Fobinso granitoids show significant enrichment in LILE such as Rb, Ba, Th and U and depletion in HFSE such as Zr, Hf, Nb and Ta. Trace elements pattern of the granitoid samples resembles the upper continental crust pattern (Rudnick and Gao, 2003). Th/U ratio of more than 2.5 of the samples further suggests the continental crust affinity as proposed for the upper continental composition (Taylor and McLennan, 1985).

A common magma source can be inferred for the Esuajah granitoids, since the Zr:Hf ratios (computed from Table 2) shows very little variations. On the other hand, Zr: Hf ratio within the Fobinso granitoids show significant variation which implies an interplay of magma fluids of different source or interaction of magma with crustal materials by the process of crustal assimilation (Yang et al., 2008). Ferromagnesian elements such as Co, Cr, Ni, Sc and V also showed marked depletion within the samples.

3.2 Geochemical constraints on tectonic regimes

The millication R1 and R2 plot (Figure 7a) identifies the Ayanfuri intrusive bodies as emplaced during an orogenic event. A group of researchers showed that granitic plutonism within the sedimentary basin are coeval with the Eburnean orogeny that affected much of the Birimian and Tarkwain (Oberthur et al., 1998). The plot of granitoid in the syn-collision region also reflects restricted anatectic two-mica granite with S-type affinity as a result of the partial melting of metasedimentary crustal material.

The sedimentary components of the magma may be carried by the descending slab during subduction (Saleh et al., 2002). This is consistent with field observation as the granitoid are hosted by metasedimentary country rocks. The trace element discrimination diagram (Figure 7b) plot samples as volcanic arc granites. Volcanic arc granites are linked to magma source depleted in mantle material that contains crustal components through the subduction process (Pearce, 1996).

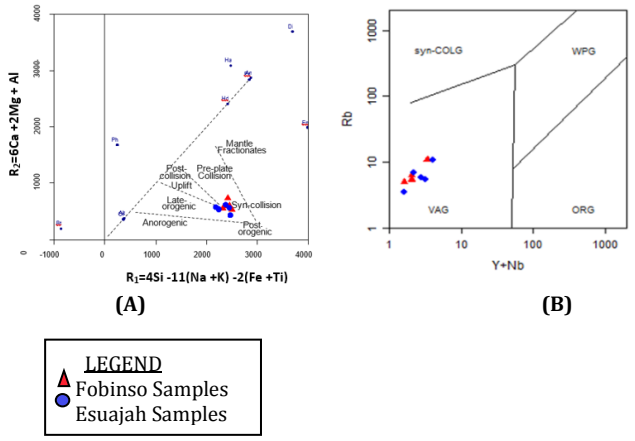

Figure 7: Tectonic discrimination diagrams a R1-R2 Millication diagram with tectonic discrimination fields b Rb vs Nb+Y tectonic discrimination diagram (Pearce et al., 1984; De La Roche et al., 1980; Batchelor and Bowden, 1985).

3.3 Gold Mineralization

Gold values in all granitoids are anomalous when compared with the highly felsic average granitoid gold value of 0.004 ppm (Turekian et al., 1961). The average values of gold in Fobinso and Esuajah samples are 0.15 ppm and 0.8 ppm respectively. The mineralized granodiorite are calc-alkaline, peraluminous intrusions of felsic composition emplaced during the Eburnean tectono-thermal orogeny that is constrained to time range of 2120 -2080 Ma (Oberthur et al., 1997). The study area is identified to have undergone a complex polyphase deformation (Figure 2) (Tourigny et al., 2018). The intrusives deformed in a brittle manner during the later stage penetrative deformational event that affected the area. This generated a network of brittle faults with contrasting kinematics under a hybrid compression stress regime (Tourigny et al., 2018). The fractures that resulted from the hybrid compression tectonic regime host auriferous quartz veins and stockworks as gold-bearing fluids infiltrate them as shown in figure (3a).

Large ion lithophile elements (LILE) (e.g., Rb, Cs, Sr and Ba) are enriched, while base metals such as Cu, Mo, Pb, Sn and Zn are within background values when compared to PM values. Enrichment of LILE can be correlated to the regional Eburnean greenschist facie metamorphism of the Kumasi supergroup country rocks (Chudasama et al., 2016). Significant amounts of LILE occur in wall rock alteration in metamorphic terranes (Grooves et al.,1998). The element suite of Au-Ag-Te-Pb-Bi-Sc-Mo-W-As-Sb which is of interest in gold exploration (Nichol, 1983), is enriched in the granitoids as compared to the primitive mantle (PM) values (Figure 6). From Table 4a and 4b, gold shows good correlation (***in bold***) with Ag-As-Bi-Sb-Te-Pb-S and Ag-As-Te-Sb-S suites, at Esuajah and Fobinso respectively. The metal associations are typical of orogenic gold deposit suite of Au-Ag ± As ± B ± Bi ± Sb ± Te ± W (Grooves et al., 2003; Robert et al., 2007; Grooves et al.,1998). From field observations, alteration minerals such as sericite and the chlorites show the pervasive alteration of the plagioclase and amphiboles respectively. According to a study, these alterations are indicators to orogenic gold deposits (Grooves et al., 1998).

Table 4: Two-tailed Pearson correlation matrix of selected elements (Significant correlation coefficients; p≤0.01 and p≤0.05, are asterisked). a. Esuajah b. Fobinso

	Ag	As	Au	Bi	Co	Cr	Cu	Fe	Mg	Mn	Mo	Ni	Pb	S	Sb	Sc	Te	Zn
Ag	1.00																	
As	.940*	1.00																
Au	**.956***	**.955***	1.00															
Bi	.909*	0.75	**0.80**	1.00														
Co	-0.77	-0.85	-.918*	-0.51	1.00													
Cr	-0.86	-0.69	-0.69	-0.87	0.40	1.00												
Cu	0.18	-0.06	-0.05	0.23	0.24	-0.63	1.00											
Fe	-.939*	-.932*	-.99**	-0.81	.915*	0.65	0.10	1.00										
Mg	-0.80	-0.84	-.937*	-0.63	.968**	0.41	0.32	.955*	1.00									
Mn	-0.78	-0.81	-.923*	-0.64	.945*	0.40	0.34	.948*	.997**	1.00								
Mo	0.23	0.26	0.01	0.21	0.24	-0.47	0.45	0.06	0.30	0.35	1.00							
Ni	-0.77	-0.85	-.923*	-0.53	.999**	0.40	0.24	.924*	.976**	.957*	0.26	1.00						
Pb	0.75	0.78	**0.87**	0.69	-0.84	-0.35	-0.45	-.909	-.945	-.962	-0.31	-0.85	1.00					
S	0.85	0.63	**0.67**	.919*	-0.36	-.98**	0.59	-0.65	-0.42	-0.42	0.36	-0.38	0.40	1.00				
Sb	.967**	.952*	**.895***	.880*	-0.68	-0.84	0.13	-0.87	-0.70	-0.68	0.42	-0.68	0.69	0.80	1.00			
Sc	-.895*	-0.85	-.894*	-.914*	0.70	0.65	0.16	.917*	0.83	0.84	-0.03	0.72	-.909	-0.70	-.879*	1.00		
Te	.970**	.886*	**.960****	.930*	-0.79	-0.79	0.07	-.97**	-0.86	-0.86	0.02	-0.80	0.85	0.81	.902*	-.947*	1.00	
Zn	-0.88	-.910*	-.97**	-0.65	.981**	0.57	0.09	.964**	.959**	.938*	0.12	.981**	-0.84	-0.54	-0.79	0.78	-.882*	1.00

	Ag	As	Au	Bi	Co	Cr	Cu	Fe	Mg	Mn	Mo	Ni	S	Sb	Sc	Te	Zn
Ag	1.00																
As	0.79	1.00															
Au	**0.75**	**.935***	1.00														
Bi	-0.50	-0.50	-0.67	1.00													
Co	-0.78	-.93*	-.936*	0.78	1.00												
Cr	-.89*	-0.87	-.895*	0.80	.969**	1.00											
Cu	-0.36	-0.50	-0.62	.962**	0.77	0.74	1.00										
Fe	-.91*	-0.87	-0.87	0.77	.956*	.996**	0.70	1.00									
Mg	-.9**	-.91*	-.880*	0.64	.922*	.968**	0.55	.978**	1.00								
Mn	-.9**	-0.79	-0.74	0.62	0.84	.934*	0.51	.958*	.970**	1.00							
Mo	-0.87	-0.83	-0.85	0.83	.952*	.996**	0.77	.994**	.953*	.937*	1.00						
Ni	-.94*	-.89*	-.893*	0.71	.943*	.987**	0.62	.991**	.996**	.964**	.976**	1.00					
S	0.52	.880*	**.907***	-0.36	-0.76	-0.64	-0.4	-0.61	-0.67	-0.46	-0.57	-0.66	1.00				
Sb	0.85	0.77	**0.63**	-0.03	-0.56	-0.61	0.07	-0.64	-0.79	-0.75	-0.56	-0.73	0.60	1.00			
Sc	-.95*	-0.88	-0.87	0.45	0.81	0.86	0.32	0.87	.950*	.896*	0.83	.927*	-0.7	-.89*	1.00		
Te	0.81	0.76	**0.83**	-.907*	-.930*	-.98**	-0.8	-.97**	-.897*	-.886*	-.99**	-.934*	0.52	0.43	-0.75	1.00	
Zn	-.89*	-.91*	-.913*	0.76	.975**	.997**	0.70	.994**	.979**	.934*	.987**	.992**	-0.7	-0.65	.887*	-.96*	1.00

4. Conclusion

The granitoids are predominantly granodiorite that has crystallized from a calc-alkaline magma series. The Esuajah and Fobinso peraluminous granodiorite are products of the anatexis of continental crustal material of igneous and metasedimentary compositions and were emplaced during a regional tectonic activity. Geochemical data is consistent with a classic orogenic model for the granitoid-hosted gold deposits. Gold is associated with As, Ag, Te, Sb, S, Bi and Pb for mineralized Esuajah rocks and As, Ag, Sb and S in the mineralized rocks of Fobinso. These elements that form an association with gold are ubiquitous in the environment and usually occur in quantities that can be recovered easily making them useful pathfinders for the gold. According to Goldfarb and Groves (2015), carbonaceous or shale-rich sequence are preferred sources of ore-forming components before remobilization into other structures for the orogenic gold deposit. Hence further research should focus on the sedimentary country-rock of the Fobinso and Esuajah intrusive as a potential source of ore-forming components.

References

Adadey, K., Clarke, B., Théveniaut, H., Urien, P., Delor, C., Roig, J.Y., Feybesse, J.L., 2009. Geological map explanation — map sheet 0503 B (1:100 000), CGS/BRGM/Geoman, Geological Survey Department of Ghana (GSD). No MSSP/2005/GSD/5a

Aitchison, J.,1982. The statistical analysis of compositional data (with discussion). Journal of the Royal Statistical Society, Series B (Statistical Methodology), 44 (2), Pp. 139-177.

Allibone, A., Heyden, P., Cameron, G., Duku, F., 2004. Paleoproterozoic gold deposits hosted by albite- and carbonate-altered tonalite in the Chirano District, Ghana, West Africa. Econ Geol., 99, Pp. 479–497.

Batchelor, R.A., Bowden, P., 1985. Petrogenetic interpretation of granitoid rock series using multicationic parameters. Chemical Geology, 48, Pp. 43-55.

Calderwood, M., Thomson, K., 2007. History of exploration: Ayanfuri gold project, Ghana. Proceedings of the NewGenGold Conference, 15-16 November, Perth, Western Australia.

Central Ashanti Gold Limited, (CAGL), 2019. Technical Report. 2011. http://www.perseusmining.com/technical_reports.60.html. 2019. 07.014

Chappell, B.W., White, A.J.R., 1974. Two contrasting granite types. Pacific Geology, 8, Pp. 173–174.

Chappell, B.W., White, A.J.R., 2001. Two contrasting granite types: 25 years later. Australian Journal of Earth Sciences, 48, Pp. 489–499.

Chudasama, B., Porwal, A., Kreuzer, O.P., Brutera, K., 2016. Geology, geodynamics and orogenic gold prospectivity modelling of the Paleoproterozoic Kumasi Basin, Ghana, West Africa. Ore Geol Rev., 78, Pp. 692–711.

De La Roche, H., Leterrier, P., Grandclaude, P., Marchal, M., 1980. A classification of volcanic and plutonic rocks using the R1-R2 diagram and major element analyses. Its relationships with current nomenclature. Chemical Geology, 29, Pp. 183-210.

Debon, F., Le Fort, P., 1983. A chemical–mineralogical classification of

common plutonic rocks and associations. Transactions of the Royal Society of Edinburgh, Earth Sciences, 73, Pp. 135–149.

Fougerouse, D., Micklewaite, S., Ulrich, S., Miller, J., Godel, B., Adams, D.T., McCuaig, T.C., 2017. Evidence for two stages of mineralization in West Africa's largest gold deposit: Obuasi, Ghana. Econ Geol., 112, Pp. 3–22.

Frost, B.R., Barnes, C.G., Collins, W.J., Arculus, R.J., Ellis, D.J., Frost, C.D., 2001. A geochemical classification for granitic rocks. Journal of Petrology, 42, Pp. 2035-2048.

Frost, B.R., Frost, C.D., 2008. A Geochemical Classification for Feldspathic Igneous Rocks. Journal of Petrology, 11, Pp. 1955-1969.

Goldfarb, R.J., Groves, D.I., 2015. Orogenic gold: Common or evolving fluid and metal sources through time, LITHOS doi: 10.1016/j.lithos.2015.07.011.

Goldfarb, R.J., Groves, D.I., Gardoll, S., 2001. Orogenic gold and geologic time: A global synthesis: Ore Geology Reviews, 18, Pp. 1–75.

Griffis, J.R., Barning, K., Agezo, F.L., Akosah, F.K., 2002. Gold deposits of Ghana. Minerals Commission.

Groves, D.I., Goldfarb, R.J., Gebre-Mariam, M., Hagemann, S.G., Robert, F., 1998. Orogenic gold deposits: A proposed classification in the context of their crustal distribution and relationship to other gold deposit types: Ore Geology Reviews, 13, Pp. 7–27.

Groves, D.I., Goldfarb, R.J., Robert, F., Hart, C.J.R., 2003. Gold Deposits in Metamorphic Belts: Overview of Current Understanding, Outstanding Problems, Future Research, and Exploration Significance. Economic Geology, 98, Pp. 1–29.

Hart, C.J.R., Goldfarb, R.J., 2005. Distinguishing intrusion-related from orogenic gold systems: Proceedings of the 2005 New Zealand Minerals Conference, Auckland, November, 13-16, Pp. 125-133.

Hart, C.J.R., Selby, D., Creaser, R.A., 2000. Timing relationships between plutonism and gold mineralization in the Tintina gold belt (Yukon and Alaska) using Re-Os molybdenite dating, in––A hydrothermal odyssey: New developments in metalliferous hydrothermal systems research: Program with abstracts: Queensland, James Cook University Townsville, Pp. 71–72.

Hirdes, W., Davis, D.W., 2002. U–Pb Geochronology of Paleoproterozoic rocks in the southern part of the Kedougou–Kéniéba Inlier, Senegal, West Africa: evidence for diachronous accretionary development of the Eburnean province. Precambrian Research, 118, Pp. 83-99.

Hirdes, W., Leube, A., 1989. On gold mineralization of the Proterozoic Birimian Supergroup in Ghana/West Africa. Bundesanstalt für Geowissenschaften und Rohstoffe, Hannover, Pp. 179.

Irvine, T.N., Baragar, W.R.A., 1971. A guide to the chemical classification of the common volcanic rocks. Canadian Journal of Earth Sciences, 8, Pp. 523-548.

Janoušek, V., Moyen, J.F., Martin, H., Erban, V., Farrow, C., 2016. Geochemical modelling of igneous processes—principles and recipes in R language. Springer Geochemistry, New York.

Jessell, M.W., Begg, G.C., Miller, M.S., 2016. The geophysical signatures of the West African Craton. Precambrian Res., 274, Pp. 3–24.

Kempe, U., Belyatsk, B.V., Krymsky, R.S., Kremenetsky, A.A., Ivanov, P.A., 2001. Sm-Nd and Sr isotope systematics of scheelite from the giant Au(-W) deposit Muruntau (Uzbekistan)-implications for the age and sources of Au mineralization: Mineralium Deposita, 36, Pp. 379-392.

Kesse, G.O., 1985 The Mineral and Rock Resources of Ghana. Balkema, Rotterdam, Pp. 610.

Leube, A., Hirdes, W., Mauer, R., Kesse, G.O., 1990. The early Proterozoic Birimian Supergroup of Ghana and some aspects of its associated gold mineralization. Precambrian Res., 46, Pp. 139-165.

Maniar, P.D., Piccoli, P.M., 1989. Tectonic discrimination of Granitoids. Geol. Soc. Amer. Bull., 101, Pp. 635–643.

Martín-Fernández, J.A., Hron, K., Templ, M., Filzmoser, P., Palarea-Albaladejo, J., 2012. Model-based replacement of rounded zeros in compositional data: Classical and robust approaches. Computational Statistics and Data Analysis, 56, Pp 2688–2704

McDonough, W.F., Sun, S.S., 1995. The Composition of the Earth. Chem. Geol., Pp. 2541.

Nichol, I., 1983. Geochemical exploration of gold, a special problem. In: Thornton, I. and Howarth (Editors), Applied Geochemistry in the 1980s. Graham and Trotman, London, Pp. 60-85.

Nude, P.M., Hanson, J.E.K., Dampare, S.B., Akiti, T.T., Osae, S., Nyarko, E.S., Zachariah, N., Enti-Brown, S., 2012. Geochemistry of pegmatites associated with the Cape Coast granite Complex in the Egyaa and Akim Oda areas of Southern Ghana. Ghana J. Sci., 51, Pp. 89-100.

Nyarko, S.E., Asiedu, D.K., Dampare, S., Zakaria, N., Hanson, J., Osei, J., Enti-Brown, S., Tulasi, D., 2012 Geochemical characteristics of the basin-type granitoids in the Winneba Area of Ghana. Proceedings of the International Academy of Ecology and Environmental Sciences, 2(3), Pp. 177-192.

Oberthur, T., Amanor, J.A.W.J., Chryssoulis, S.L., 1997. Mineralogical siting and distribution of gold in quartz veins and sulfide ores of the Ashanti mine and other deposits in the Ashanti belt of Ghana: genetic implications. Meneralium Depos., 32, Pp. 2–15.

Oberthür, T., Vetter, U., Davis, D.W., Amanor, J.A., 1998. Age constraints on gold mineralisation and Paleoproterozoic crustal evolution in the Ashanti belt of southern Ghana. Precambrian Research, 89, Pp. 129-143.

Palarea-Albaladejo, J., Martín-Fernández, J.A., Gómez-García J., 2007. A Parametric Approach for Dealing with Compositional Rounded Zeros. Mathematical Geology, 39, Pp. 625–645.

Pearce, J.A., 1996. A user's guide to basalt discrimination diagrams. In: WYMAN, D. A. (ed.): Trace Element Geochemistry of Volcanic Rocks: Applications for Massive Sulphide

Pearce, J.A., Harris, N.B.W., Tindle, A.G., 1984. Trace elememnt discrimination diagrams for the tectonic interpretation of granitic rocks. Journal of petrology, 25, Pp. 217-235.

Peccerillo, A., Taylor, S.R., 1976. Geochemistry of Eocene calc-alkaline volcanic rocks from the Kastamonu area, Northern Turkey. Contributions to Mineralogy and Petrology, 58, Pp. 63-81.

Perrouty, S., Aillères, L., Jesselll, M.W., Baratoux, L., Bourassa, Y., Crawford, B., 2012. Revised Eburnean geodynamic evolution of the gold-rich southern Ashanti belt, Ghana, with new field and geophysical evidence of pre-Tarkwaian deformation. Precambrian Res., 204-205, Pp. 12–39.

Robert, F., Brommecker, R., Bourne, B.T., Dobak, P.J., McEwan, C.J., Rowe, R.R., Zhou, X., 2007. Models and Exploration Methods for Major Gold Deposit Types. In "Proceedings of Exploration 07: Fifth Decennial International Conference on Mineral Exploration" edited by B. Milkereit, Pp. 691-711.

Rudnick, R.L., Gao, S., 2003. Composition of the Continental Crust. Treatise on Geochemistry 3, 1-64 (eds. H.D. Holland and K.K. Turekian), Elsevier-Pergamon, Oxford.

Saleh, G.M., Dawood, Y.H., Abd El-Naby, H.H., 2002. Petrological and geochemical constraints on the origin of the granitoid suite of the Homret Mikpid are South Eastern Desert, Egypt. Journal of Mineralogical and Petrological Sciences, 97, Pp. 47-58.

Santisteban, J.I., Dabrio, C.J., Mediavilla, R., Lo, E., Garcı, G., Castan, S., Zapata, M.B.R., Jose, M., Mart, P.E., 2004. Loss on ignition: a qualitative or quantitative method for organic matter and carbonate mineral content in sediments. J. Paleolimnol., 32, Pp. 287–299.

Schmidt Mumm, A., Oberthür, T., Vetter, U., Blenkinsop, T.G., 1997. High CO2 content of fluid inclusions in gold mineralizations in the Ashanti Belt, Ghana: a new category of ore-forming fluids? Mineralium Deposita, 32, Pp. 107-118.

Shand, S.J., 1943. Eruptive Rocks. Their Genesis, Composition, Classification, and Their Relation to Ore-Deposits with a Chapter on Meteorite. John Wiley & Sons, New York.

Sillitoe, R.H., 1991. Intrusion-related gold deposits, in Foster RP ed., Gold metallogeny and exploration: Glasgow, Blackie and Son, Ltd., Pp. 165–209.

Taylor, S.R., McLennan, S.M., 1985. The Continental Crust: Its Composition and Evolution. Blackwell, Oxford.

Tourigny, G., Tranos, M.D., Masurel, Q., 2018. Structural controls on granitoid-hosted gold mineralization and paleo stress history of the Edikan gold deposits, Kumasi Basin, southwestern Ghana. Mineralium Deposita.

Turekian, K.K., Wedepohl, K.H., 1961. Distribution of the Elements in Some Major Units of the Earth's Crust. Geological Society of America Bulletin, 72, Pp. 175-192.

Wilson, M., 1989. Igneous Petrogenesis. Unwin Hyman, London.

Wirth, K., Barth, A., 2016. Geochemical Instrumentation and Analysis (XRF): http://serc.carleton.edu/research. 03. 0.18.

Yang, X., Lentz, D.R., Chi, G., Thorne, K.G., 2008. Geochemical characteristics of gold-related granitoids in southwestern New Brunswick, Canada Lithos, 104, Pp. 355–377.

Yao, Y., Murphy, P.J., Robb, L.J., 2001, Fluid Characteristics of Granitoid-Hosted Gold Deposits in the Birimian Terrane of Ghana: A Fluid Inclusion Microthermometric and Raman Spectroscopic Study. Economic Geology, 96, Pp. 1611–1643.

Yao, Y., Robb, L.J., 2000. Gold mineralization in Palaeoproterozoic granitoids at Obuasi, Ashanti Region, Ghana: Ore geology, geochemistry and fluid characteristics. South African Journal of Geology, 103, Pp. 255-278.